The Response of Daily Carbon Dioxide and Water Vapor Fluxes to Temperature and Precipitation Extremes in Temperate and Boreal Forests

Daria Gushchina[1], Maria Tarasova [1], Elizaveta Satosina [1,2], Irina Zheleznova [1], Ekaterina Emelianova [1,2], Ravil Gibadullin [1], Alexander Osipov [1] and Alexander Olchev [1,*]

[1] Department of Meteorology and Climatology, Faculty of Geography, Lomonosov Moscow State University, GSP−1, Leninskie Gory, 1, 119991, Moscow, Russia; dasha155@mail.ru (D.G.), mkolennikova@mail.ru (M.T.), lisan.sat@gmail.com (E.S.), zheleznovaiv@my.msu.ru (I.Z.); katikget@yandex.ru (E.E.), ravil00121@mail.ru (R.G.), sashaosipov@list.ru (S.O.), aoltche@gmail.com (A.O.)
[2] A.N. Severtsov Institute of Ecology and Evolution, Russian Academy of Science, Leninsky Prospekt 33, Moscow 119071, Russia.
*Correspondence: aoltche@gmail.com

Supplementary materials

S1. Comparisons of daily temperature from ERA5 reanalysis and FLUXNET data sets.

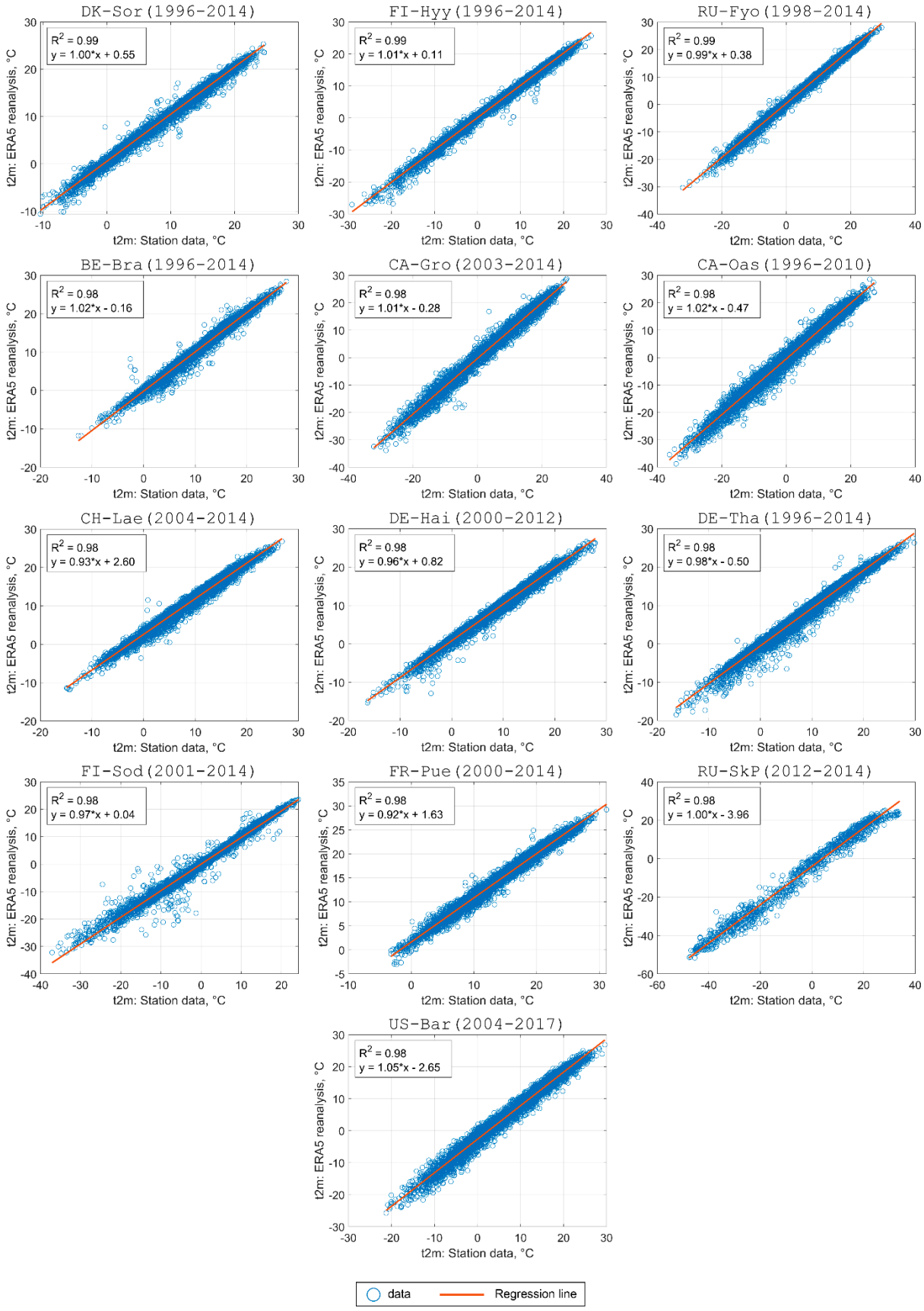

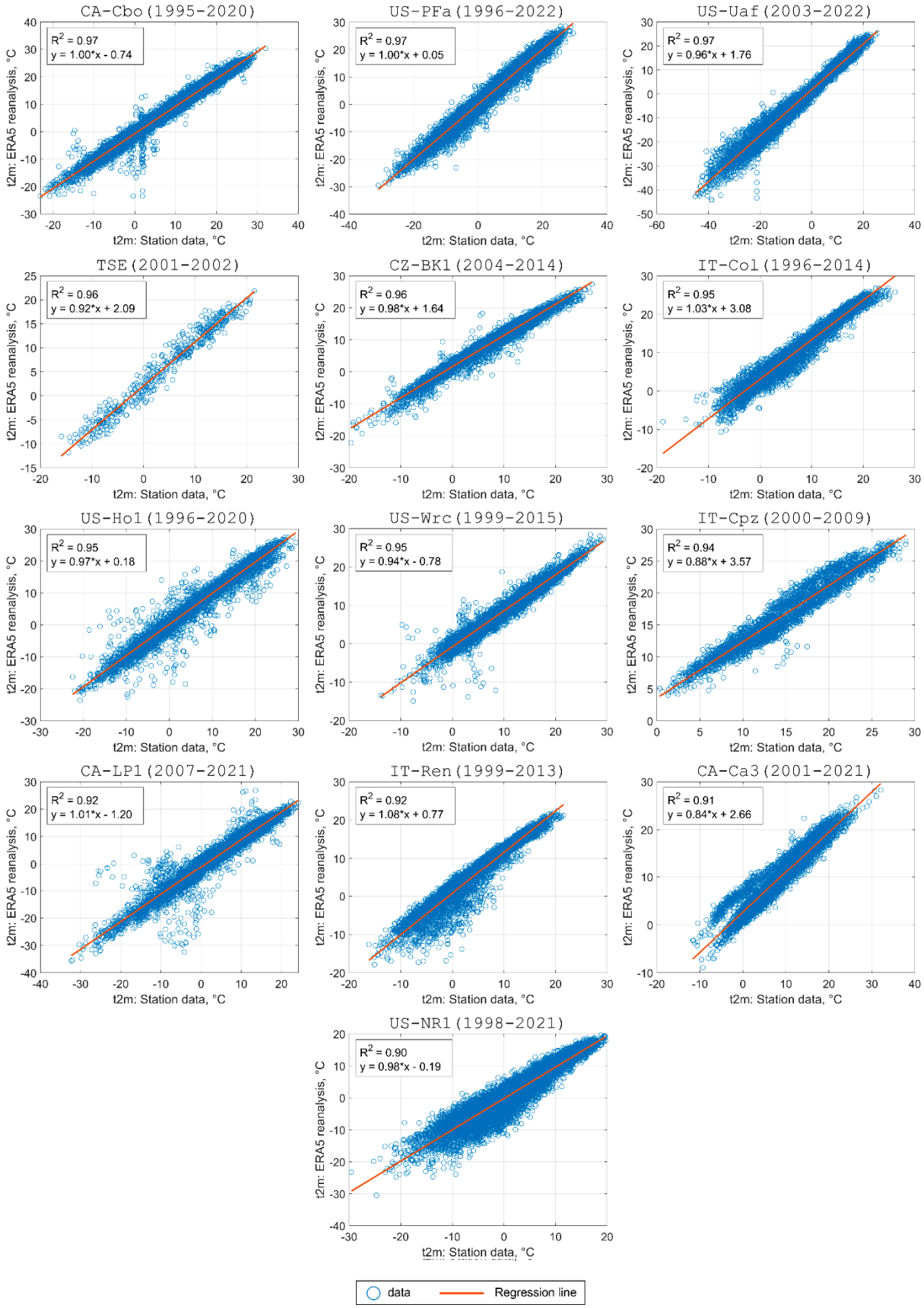

Figure S1.1: Scatter plots for analyzed stations of daily temperature from ERA5 reanalysis versus FLUXNET data sets. The period is given in brackets in the plot title.

S2. Statistical analysis of temperature and precipitation trends.

The sequential version of the Mann-Kendall test statistic (SeqMK-test) (Chatterjee, 2014, Sneyres, 1990, Mohsin and Gough, 2009) was used to estimate the trend change in the time series. The method can be used to determine whether a time series has a monotonic upward or downward trend. In addition, the method allows to identify the trend turning points in the time series (e.g. air temperature and precipitation). The SeqMK test is calculated using the ranking values yi of the initial time series (x_1, x_2, ..., x_n). Values y_i (i=1, 2, 3, ..., n) are compared with y_j (j=1,2,3,..., i-1). At each step i, the condition $y_i > y_j$ is checked and the result of this condition is stored in n_i. The t-value is determined according to Saffari (Safari, 2012) as :

$$t_i = \sum_{j=1}^{i} n_i \quad (1)$$

The distribution of test statistic t_i, is derived as:

$$E(t_i) = \frac{i(i-1)}{4} \quad (2)$$

and the variance as:

$$var(t_i) = \frac{i(i-1)(2i+5)}{72} \quad (3)$$

For each t_i, the sequential values of a reduced or standardized variable $u(t_i)$ are calculated as (4):

$$u(t_i) = \frac{t_i - E(t_i)}{\sqrt{var(t_i)}} \quad (4)$$

The forward sequence $u(t_i)$ are calculated based on the original time series (x1,x2,...,xn). The values of the backward sequence $u'(t_i)$ are evaluated in the same way, but starting from the end of the time series. When evaluating $u'(t_i)$, the time series is constructed so that the last value in the original time series is the first.

The intersection of the curves corresponding to $u(t_i)$ and $u'(t_i)$ allows the beginning of the probable trend change to be identified. If the values of $u(t_i)$ and $u'(t_i)$ at the point of change do not exceed 1.96, we can say that there is a significant change in the trend (at the 5% level of significance).

If at least one value of a reduced variable is greater than the selected significance level of the Gaussian distribution, then the null hypothesis (that the examined series has no significant trend change) is rejected.

The forward and backward sequences are calculated based on the mean annual temperature and precipitation values for the period 1980-2021 for all ERA5 grid points north of 40 N (Figure S2) and separately for the grid cells with detected trend turning point (Figure S3).

Despite the detected trend changes at individual grid points and regions, the averaging over all grid cells located at temperate and high latitudes in the Northern Hemisphere (north of 40N) does not detect the trend turning points in temperature and precipitation (the plots $u(t_i)$ and $u'(t_i)$ do not intersect). Even if the averaging is applied to the grid cells with detected trend turning points (Figure S3), it is impossible to identify the common turning point for all grid cells. For precipitation in 2015 and for temperature in 1996-1997, we see a convergence of the curves $u(t_i)$ and $u'(t_i)$, but they do not overlap. This indicates the regional variations of the detected trend changes and makes it impossible to identify the periods with significantly different trends for the whole Northern Hemisphere.

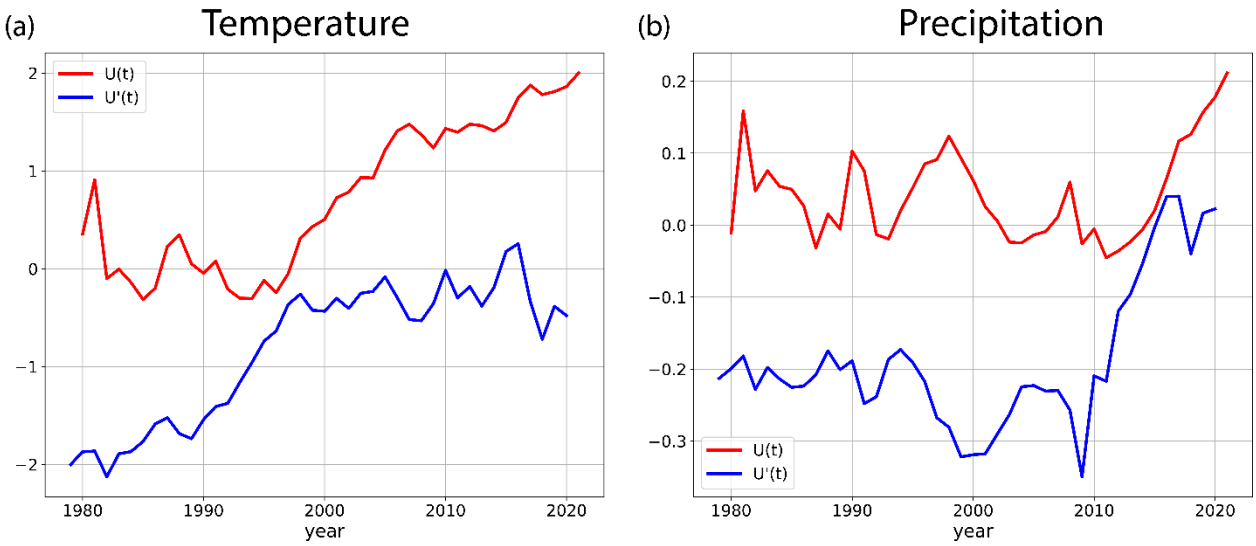

Figure S2.1 Sequential Mann-Kendall test for the air temperature (a) and precipitation (b) for all grid points situated north of 40N.

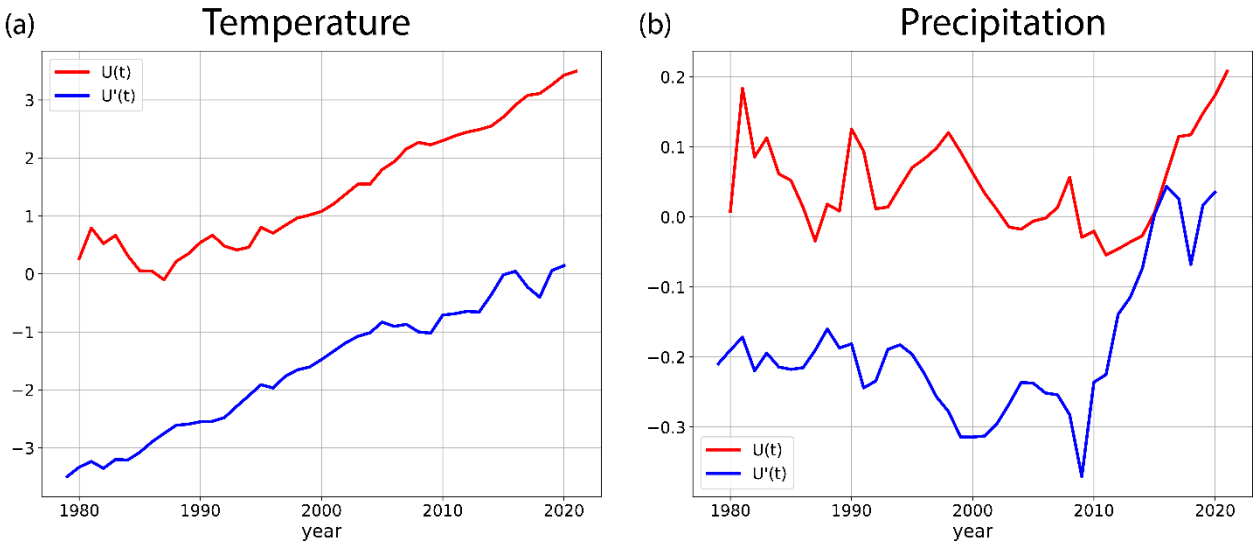

Figure S2.2 Sequential Mann-Kendall test for the air temperature (a) and precipitation (b) for grid cells with detected trend turning points situated north of 40N.

References

Chatterjee S., Bisai D., Khan A. Detection of Approximate Potential Trend Turning Points in Temperature Time Series (1941-2010) for Asansol Weather Observation Station, West Bengal, India, *Atmospheric and Climate Sciences*, 4(1), 2014, 64-69. doi: 10.4236/acs.2014.41009.

Sneyres R. On the statistical Analysis of Time Series of Observation, Technical Note No. 143, World Meteorological Organisation, Geneva, 1990.

Mohsin T. and Gough W.A. Trend Analysis of Long Term Temperature Time series in the Greater Toronto Area (GTA), *Theoretical and Applied Climatology*, 101, 2009, 311-327.

Safari B. Trend Analysis of Mean Annual Temperature in Rwanda during Last Fifty Two Years, *Journal of Environmental Protection*, 3(6), 2012, 538-551. http://dx.doi.org/10.4236/jep.2012.36065

S3. Temporal variability of daily temperature anomalies, precipitation, NEE and LE anomalies.

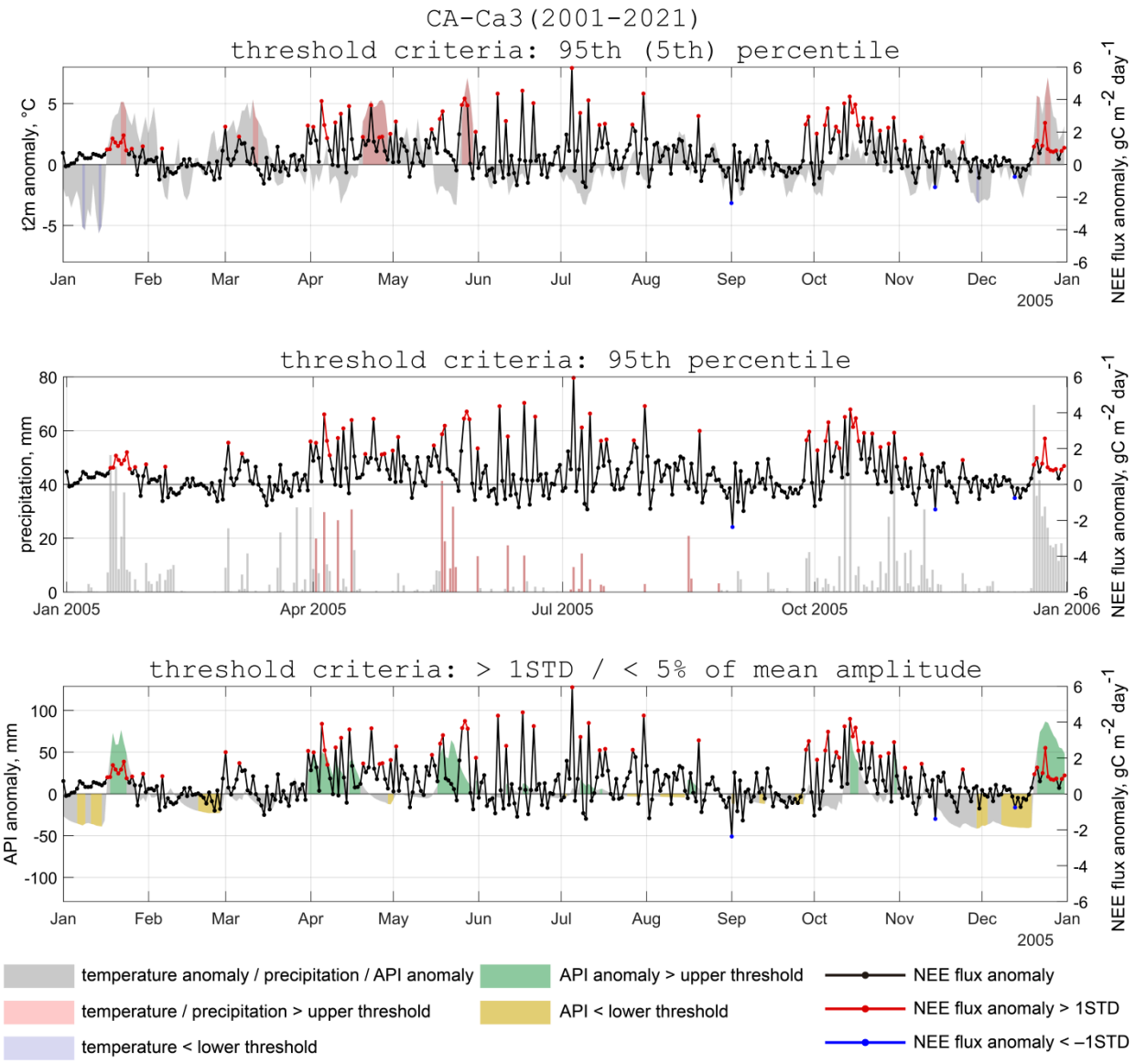

Figure S3.1

Temporal variability of daily temperature anomalies, precipitation, API, and NEE and LE flux anomalies for the evergreen needleleaf forest of western Canada (CA-Ca3).

S4. Relationships between daily NEE anomalies and daily air temperatures.

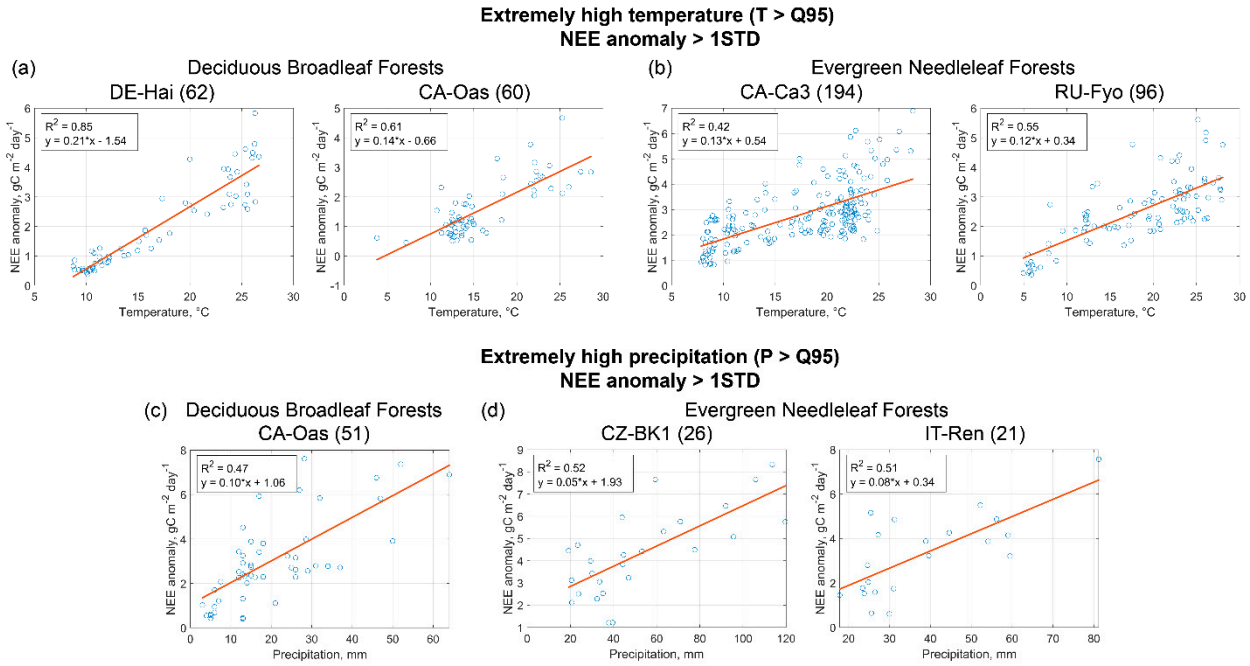

Figure S4.1 Relationships between daily NEE anomalies and daily extremely high air temperature, T > Q95 (a,b) and precipitation, P > Q95 (c,d) for selected flux stations in deciduous broadleaf (a,c) and evergreen needleleaf (b,d) forest types.

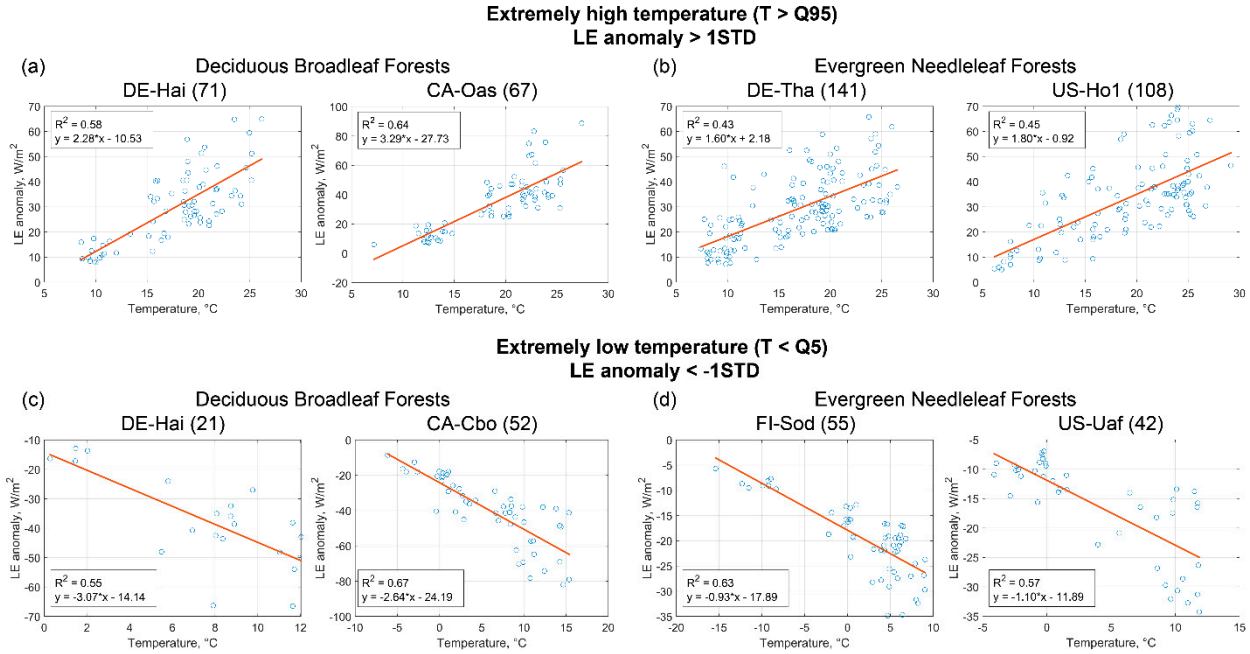

Figure S4.2 Relationships between daily positive (a,b) and negative (c,d) LE anomalies and daily extremely high (T > Q95) and low (T < Q5) air temperature for selected flux stations in deciduous broadleaf (a,c) and evergreen needleleaf (b,d) forest types.

S5. Relationships between daily NEE and air temperature anomalies.

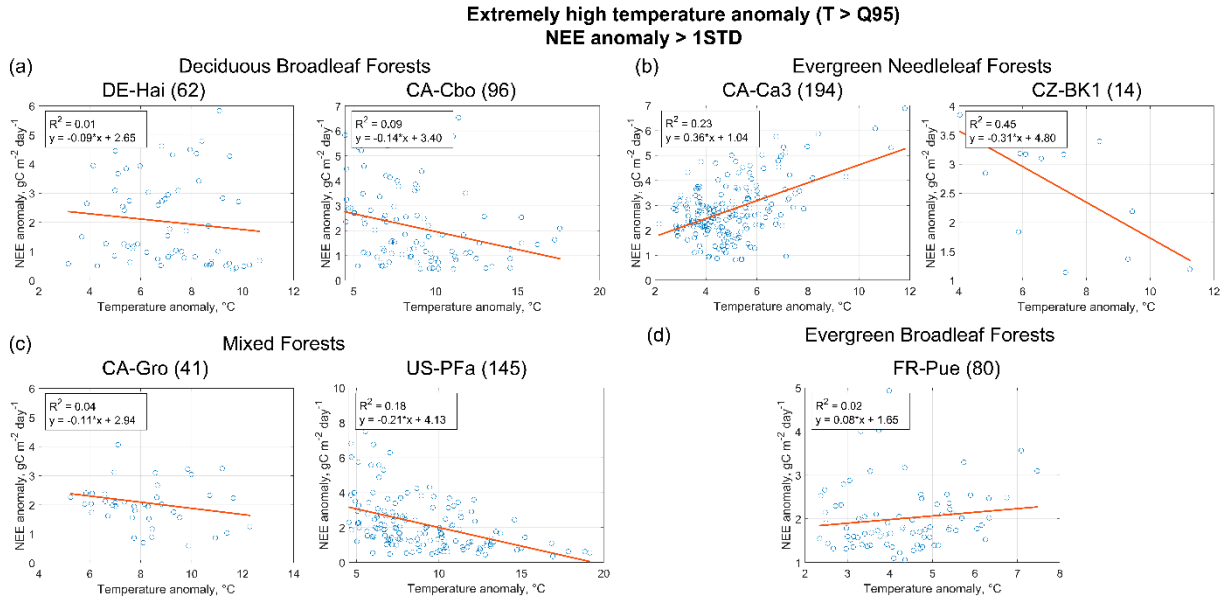

Figure S5.1 Relationships between daily positive NEE (NEE anomalies > 1 STD) and positive air temperature (T > Q95) anomalies for selected flux stations in deciduous broadleaf (a), evergreen needleleaf (b), mixed (c) and evergreen broadleaf (d) forests.

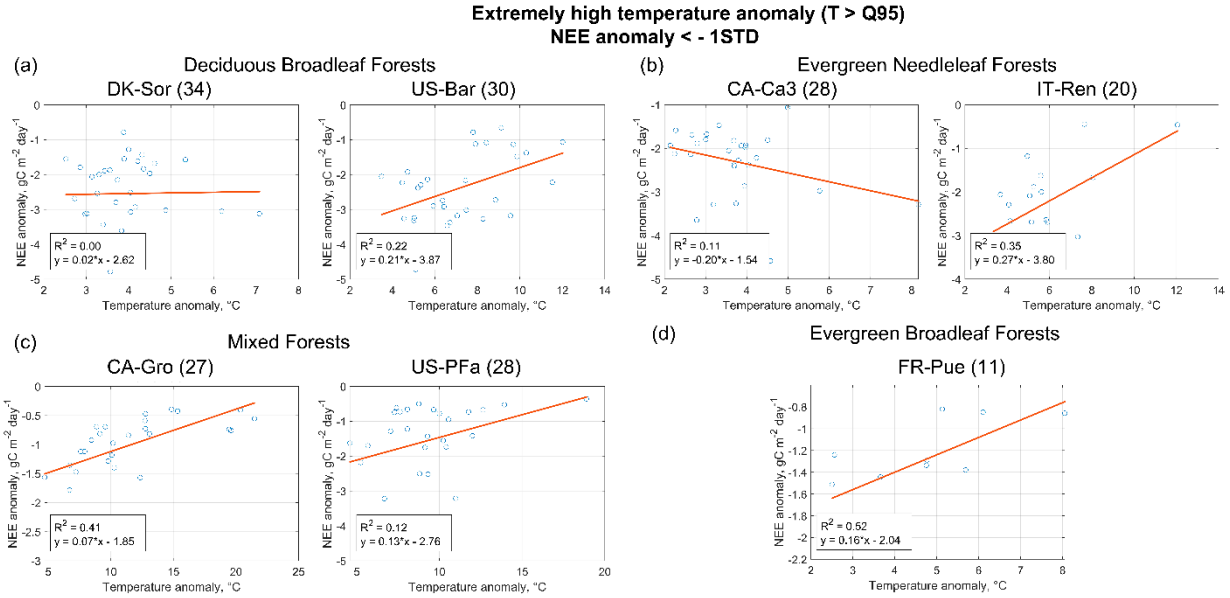

Figure S5.2 Relationships between daily negative NEE (NEE anomalies < -1 STD) and positive air temperature (T > Q95) anomalies for selected flux stations in deciduous broadleaf (a), evergreen needleleaf (b), mixed (c) and evergreen broadleaf (d) forests.

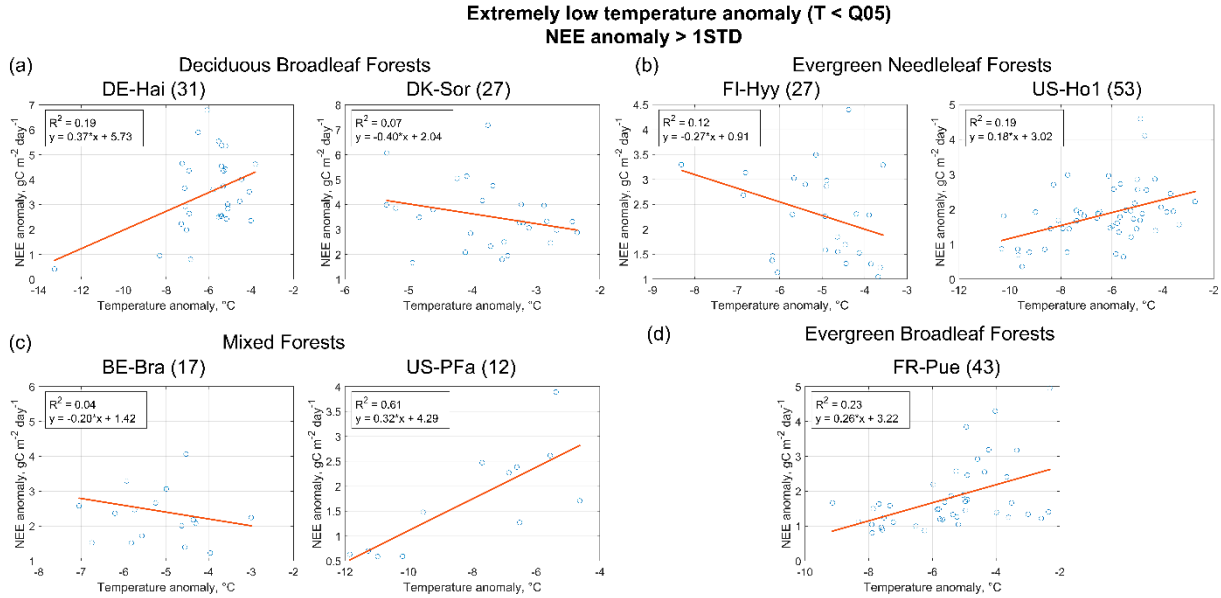

Figure S5.3 Relationships between daily positive NEE (NEE anomalies > 1 STD) and negative air temperature (T < Q05) anomalies for selected flux stations in deciduous broadleaf (a), evergreen needleleaf (b), mixed (c) and evergreen broadleaf (d) forests.

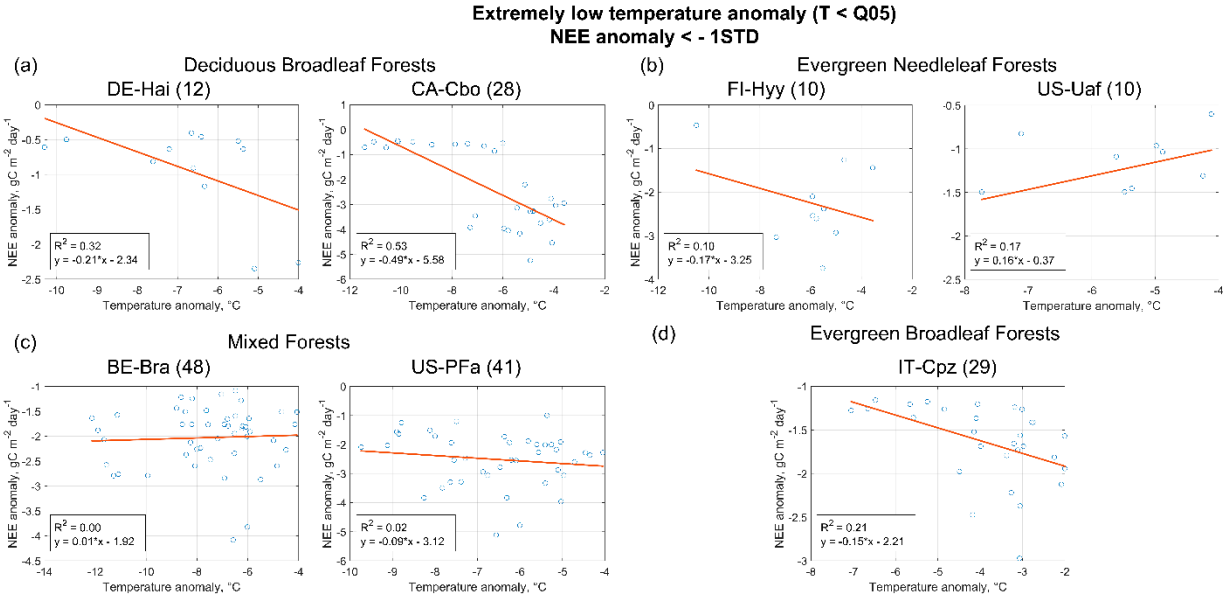

Figure S5.4 Relationships between daily negative NEE (NEE anomalies < -1 STD) and negative air temperature (T < Q05) anomalies for selected flux stations in deciduous broadleaf (a), evergreen needleleaf (b), mixed (c) and evergreen broadleaf (d) forests.

S6. Relationships between daily NEE and LE anomalies and daily extreme precipitation.

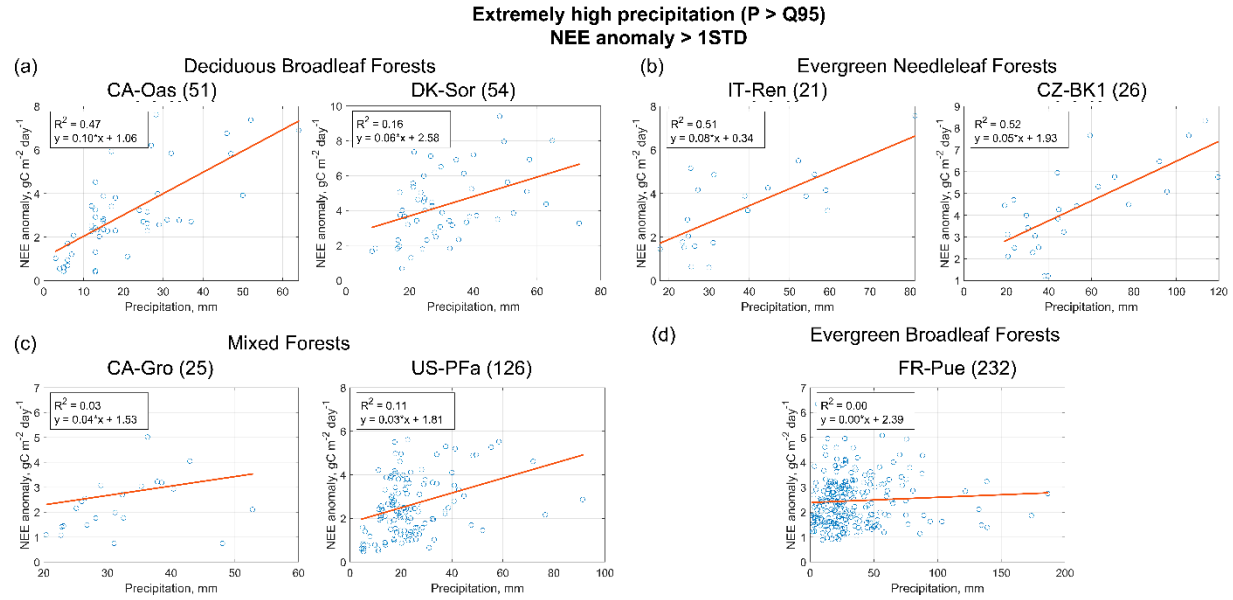

Figure S6.1 Relationships between daily positive NEE anomalies (NEE anomalies > 1 STD) and daily extreme precipitation (P > Q95) for selected flux stations in deciduous broadleaf (a), evergreen needleleaf (b), mixed (c) and evergreen broadleaf (d) forests.

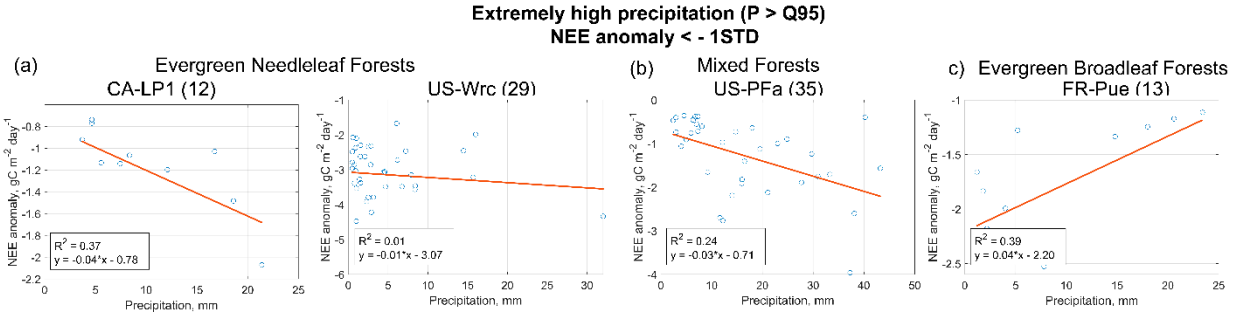

Figure S6.2 Relationships between daily negative NEE anomalies (NEE anomalies < -1 STD) and daily extreme precipitation (P > Q95) for selected flux stations in deciduous broadleaf (a), mixed (b) and evergreen broadleaf (c) forests.

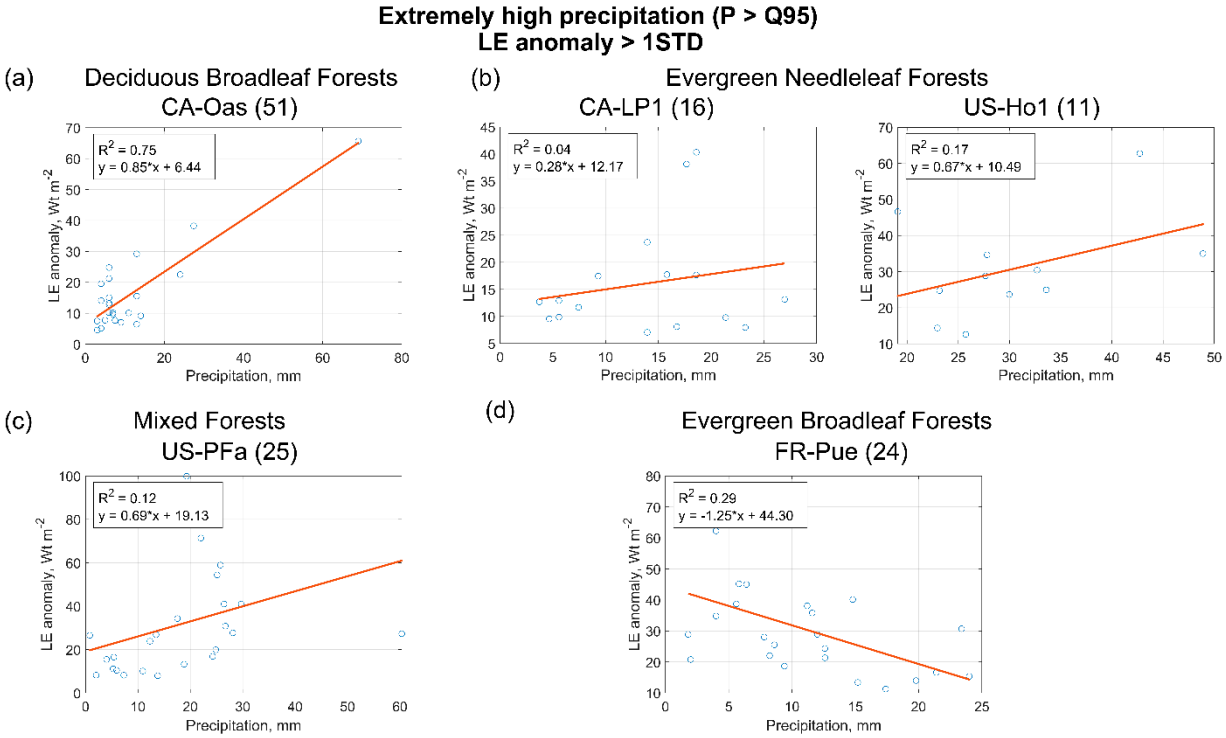

Figure S6.3 Relationships between daily positive LE flux anomalies (LE anomalies > 1 STD) and daily extreme precipitation (P > Q95) for selected flux stations in deciduous broadleaf (a), evergreen needleleaf (b), mixed (c) and evergreen broadleaf (d) forests.

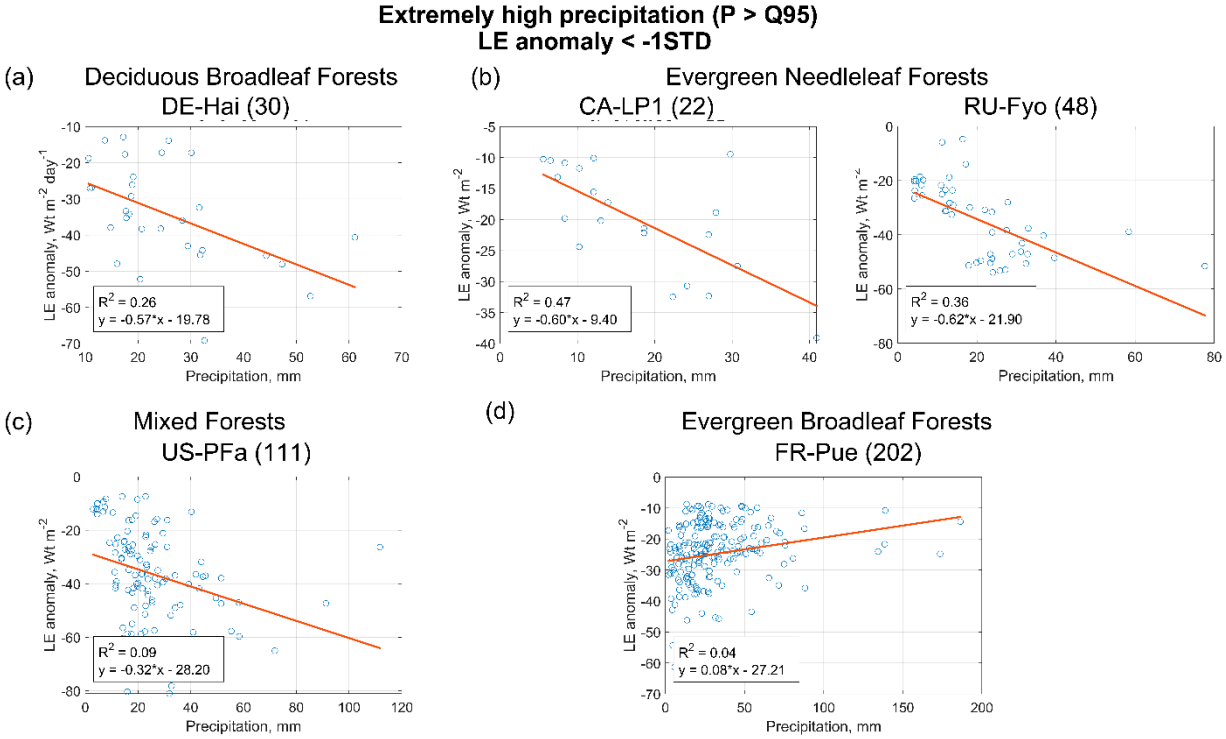

Figure S6.4 Relationships between daily negative LE flux anomalies (LE anomalies < -1 STD) and daily extreme precipitation (P > Q95) for selected flux stations in deciduous broadleaf (a), evergreen needleleaf (b), mixed (c) and evergreen broadleaf (d) forests.